Supplementary Material

Z-scheme $Mo_2C/MoS_2/In_2S_3$ Dual-heterojunction for Photocatalytic Reduction of Cr(VI)

Xin Zhang[a, 1], Fenyang Tian [a,1], Longyu Qiu[a, 1], Manyi Gao[a], Weiwei Yang[a*], Yequn Liu[b], Yongsheng Yu[a*]

[a]MIIT Key Laboratory of Critical Materials Technology for New Energy Conversion and Storage, School of Chemistry and Chemical Engineering, Harbin Institute of Technology, Harbin, Heilongjiang 150001, China.

[b]Institutional Center for Shared Technologies and Facilities of Institute of Coal Chemistry, CAS, State Key Laboratory of Coal Conversion, Taiyuan 030001, China

*To whom correspondence should be addressed. Email: yangww@hit.edu.cn, and ysyu@hit.edu.cn

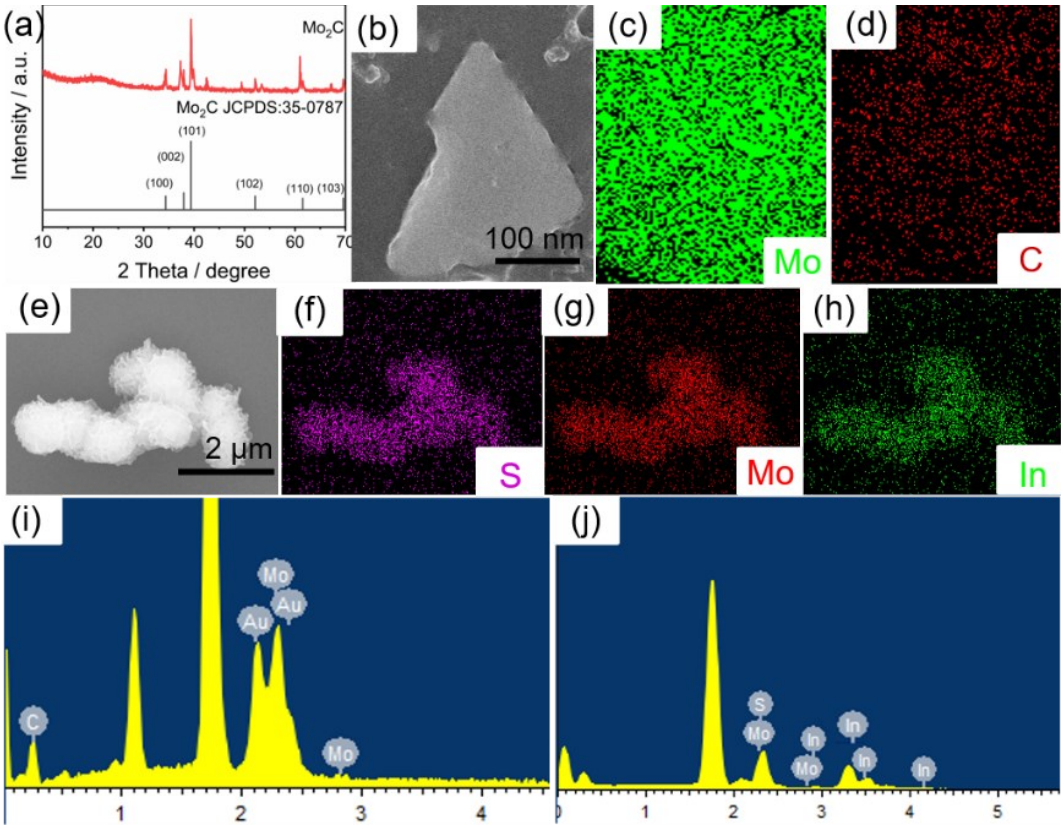

Figure S1. (a) XRD pattern of Mo_2C. (b) FESEM image of MNs and mappings of Mo (c) and C (d). (e) FESEM image of MIS and mappings of S (f), Mo (g) and In (h), (b) EDS images of MNs (i) and MIS (j).

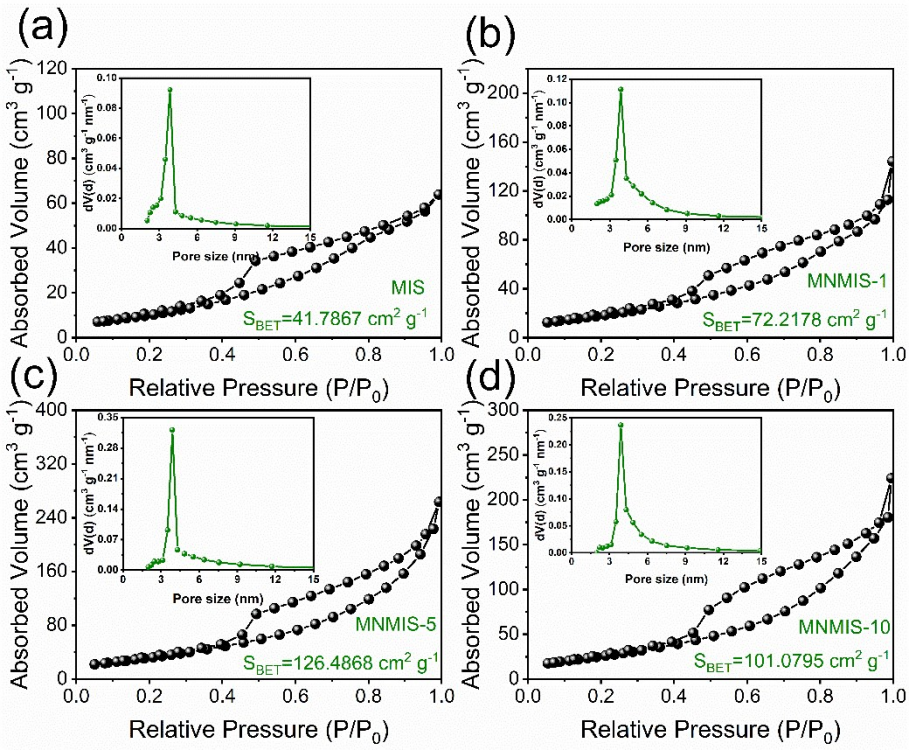

Figure S2. N_2 adsorption-desorption isotherms and corresponding pore size distribution curves (inset) of MIS, MNMIS-1, MNMIS-5 and MNMIS-10 heterojunctions.

Table S1. Specific surface area, pore volume of as-prepared samples.

Sample	S_{BET} / (m^2 g^{-1})	Pore volume / (mg L^{-1})
MIS	41.7867	0.09888
MNMIS-1	72.2178	0.2229
MNMIS-5	126.4868	0.4077
MNMIS-10	101.0795	0.3464

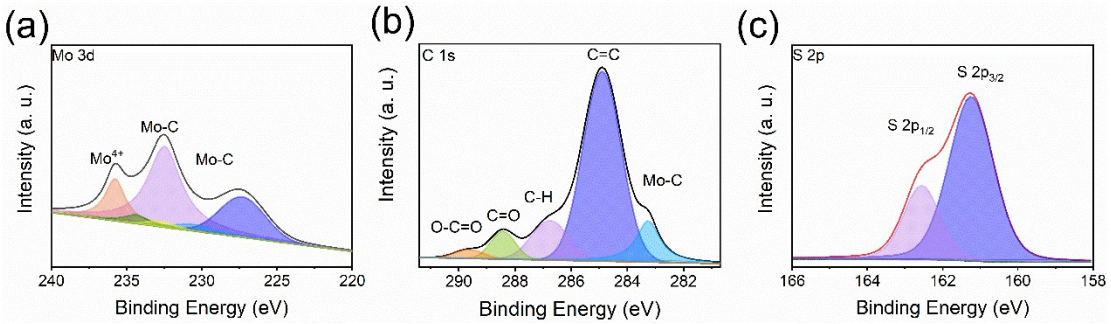

Figure S3. High-resolution XPS of Mo 3d, C 1s and S 2p spectra of MNMIS-5 heterojunction.

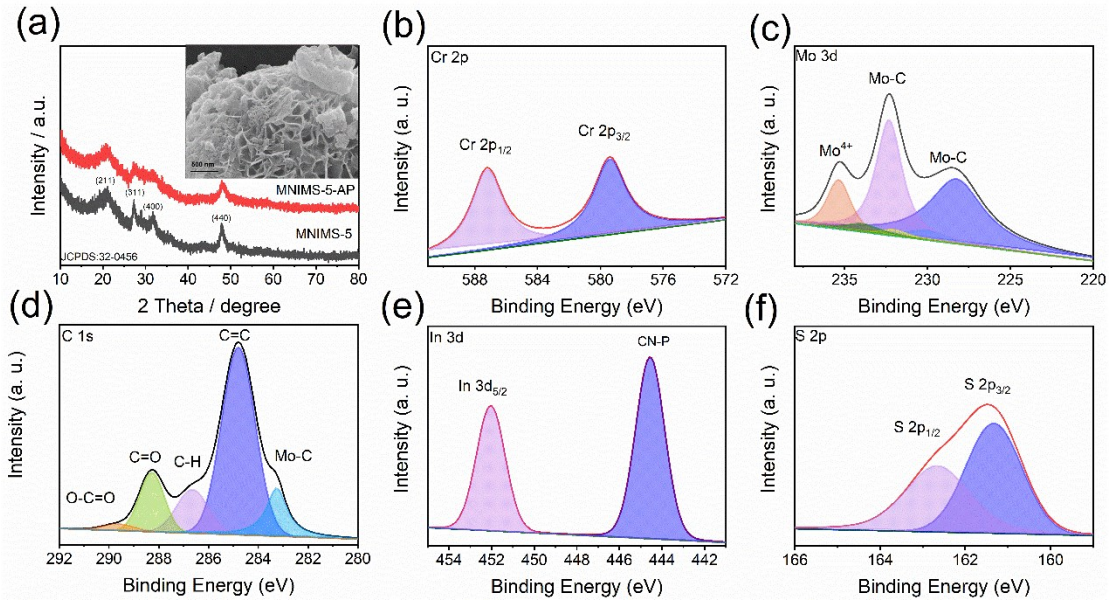

Figure S4. (a) XRD pattern of MNMIS-5 and MNMIS-5-AP and SEM image of MNMIS-5-AP (insert). High-resolution XPS of (b) Cr 2p, (c) Mo 3d, (d) C 1s, (e) In 3d and (f) S 2p spectra of MNMIS-5-AP.